Forum Acusticum 2011 - Aalborg - Denmark

Simulating transient scattering from obstacles with frequency-dependent surface impedance

J. A. Hargreaves

Acoustics research centre, University of Salford, Salford, Greater Manchester, M5 4WT, UK

Summary

This paper presents an algorithm which couples the time domain Boundary Element Method (BEM) with a digital filter surface model. This aims to achieve the same for transient sounds as is possible for time-harmonic excitation using surface impedance and the frequency domain BEM. Accurate representation of surface properties is crucial in obtaining realistic simulations, and the obstacles and boundaries typically encountered in real-world scenarios exhibit frequency-dependent surface impedance. In the time domain such frequency-dependency can be modelled using digital filters, and by this approach surface-impedance has been successfully incorporated into some recent Finite Difference Time Domain (FDTD) models, but the best way of achieving this for time domain BEM is currently unresolved. The surface model used herein uses a digital filter to implement the surface reflection coefficient – the accuracy of this approach for non-normal incidence plane waves has previously been questioned in the FDTD literature, so this scenario is specifically investigated and accuracy is evaluated by comparison with the analytical plane wave pressure reflection coefficient. Computational cost and effect on algorithm stability are also considered.

PACS no. 43.20.Fn, 43.20.Px

1. Introduction

The Boundary Element Method (BEM) has been shown to be an excellent choice for simulation in Room Acoustics, particularly when the priority is to predict scattering from small objects extremely accurately [1]. BEM requires that only the boundaries between obstacles and air are modelled as it is known how sound travels unobstructed. This produces smaller, simpler meshes compared to volumetric methods, such as finite element method and Finite Difference Time Domain (FDTD), and permits an unbounded volume of air to be modelled, making it ideal for free-field scattering scenarios. Most BEMs assume time-harmonic excitation so the unknowns are time invariant and complex. Whilst this frequency domain analysis is a useful tool, the transient behaviour witnessed in the real world may only be recovered by solving many frequency domain models and then applying an inverse discrete Fourier transform. Applications such as auralisation have thus driven an interest in time domain modelling and many geometric algorithms, and more recently FDTD, have been published in pursuit of this. The time harmonic assumption may also be dropped from the BEM formulation, leading to the time domain BEM studied here. This approach was first published by Friedman and Shaw in 1962 [2], however computational cost and stability issues have plagued the method and commercial implement-ations have appeared only very recently [3].

To achieve realistic simulations, obtaining accurate representation of surface properties is crucial. The obstacles and boundaries typically encountered in real-world scenarios are non-rigid and exhibit frequency-dependent behaviour. Surface impedance is typically used to characterise this for time-harmonic excitation and is ideally suited to use with the frequency domain BEM; an equivalent time domain model is sought. Differential boundary conditions may be used to model simple compliant materials such as frequency-invariant absorption [4,5] and limp membranes [6], but finding such models from arbitrary surface impedance data is more complicated [7]. Instead, various researchers

tackling this challenge for FDTD have turned to digital filter representations [8,9,10] and this paper investigates whether the same approach will work with time domain BEM.

2. Boundary Integral Formulation

A BEM to model scattering of sound from an object has three distinct phases: first the sound incident on the object is calculated, then the total sound at the surface of the object is solved for by considering the mutual interactions between parts of the surface *S*, and finally the scattered sound is calculated from this total surface sound. The scattered sound arising as a consequence of total sound on a surface is described by the Kirchhoff Integral Equation (KIE); this is the foundation of the time domain BEM:

$$\varphi_s(\mathbf{x},t) = \iint_S \begin{bmatrix} \varphi_t(\mathbf{y},t) * \hat{\mathbf{n}}_\mathbf{y} \cdot \nabla_\mathbf{y} g(R,t) \\ - g(R,t) * \hat{\mathbf{n}}_\mathbf{y} \cdot \nabla_\mathbf{y} \varphi_t(\mathbf{y},t) \end{bmatrix} d\mathbf{y} \qquad (1)$$

$$p(\mathbf{x},t) = -\rho_0 \dot{\varphi}(\mathbf{x},t) \qquad (2)$$

$$\mathbf{v}(\mathbf{x},t) = \nabla \varphi(\mathbf{x},t) \qquad (3)$$

x and **y** are 3D Cartesian vectors defining the observation and radiation points respectively and $R = |\mathbf{x} - \mathbf{y}|$ is the distance between them. φ represents velocity potential, a non-physical quantity from which pressure and velocity may be derived according to equations 2 and 3, where ρ_0 and c are the density of and speed of sound in air respectively. A dot above a quantity represents temporal differentiation and temporal convolution is represented by $*$. φ_s is the scattered sound and φ_t is the total sound. $\hat{\mathbf{n}}_\mathbf{y}$ is the surface normal vector at **y** and $g(R,t)$ is the time domain Green's function which describes how sound travels from a point source to an observer, which intuitively comprises a delay term as a numerator ($\delta(\ldots)$ is the dirac delta function) and a reduction in magnitude with distance as the denominator:

$$g(R,t) = \frac{\delta(t - R/c)}{4\pi R} \qquad (4)$$

If the limit is taken as **x** approaches *S* from the inside of the scatterer then a solution for total surface sound φ_t may be found which eliminates the incident field. However, rather than use this scheme directly it has been shown [11,12] that stability may be improved by using a variant called the Combined Field Integral Equation (CFIE):

$$(1-\alpha) p_t(\mathbf{x},t) = \alpha \rho_0 c \hat{\mathbf{n}}_\mathbf{x} \cdot \mathbf{v}_t(\mathbf{x},t). \qquad (5)$$

where α typically equals ½. This is equivalent to the frequency domain Burton and Miller method [13] when an imaginary coupling parameter is used and can be shown to eliminate cavity resonances by permitting any wave emanating from inside the obstacle to pass without reflection.

3. Surface Reflectance Model

In time harmonic models the concept of surface impedance conveniently abstracts the behaviour of the material into a frequency dependent complex scalar, defined at the ratio of total pressure to the inward component of total particle velocity at any point on the surface:

$$Z(\omega) = P_t(\mathbf{x},\omega) / V_{t,in}(\mathbf{x},\omega) \qquad (6)$$

The same relationship may be stated in the time domain as $p_t(\mathbf{x},t) = v_{t,in}(\mathbf{x},t) * z(t)$. However, due to the aggregation of cause and effect in the quantities p_t and $v_{t,in}$, an impedance kernel $z(t)$, found by inverse discrete Fourier transform of $Z(\omega)$, is typically non-compact in time and requires future values of $v_{t,in}(\mathbf{x},t)$. This issue can be avoided by including convolutions on both sides of the boundary condition equation:

$$p_t(\mathbf{x},t) * b^Z(t) = v_{t,in}(\mathbf{x},t) * a^Z(t) \qquad (7)$$

This amounts to splitting the surface impedance into the quotient of two functions, which can be chosen so that they are bounded and transform to temporally compact convolution kernels. However it is still non-trivial to establish whether these frequency domain functions describe a casual and passive (energy absorbing) reflection process, and it has been suggested that a convolution between waves travelling perpendicularly into and out of the body may be a more robust approach [14]. The author has previously implemented this concept for time domain BEM for the special case of obstacles with wells that are narrow with respect to wavelength [15]. This boundary condition may be written in the time domain as:

$$\varphi_{out}(\mathbf{x},t) = \varphi_{in}(\mathbf{x},t) * w(t) \qquad (8)$$

Here $w(t)$ will be referred to as the surface reflection kernel, and its equivalent frequency quantity $W(\omega)$ the surface reflection coefficient:

$$\Phi_{out}(\mathbf{x},\omega) = \Phi_{in}(\mathbf{x},\omega)W(\omega) \qquad (9)$$

Causality and passivity of the reflection process may be readily verified by respectively ensuring that $w(t) = 0$ for $t < 0$ and $|W(\omega)| \leq 1$ for all ω. The term "surface" and the notation $W(\omega)$ have been used here to differentiate this quantity from the widely used plane wave pressure reflection coefficient $R(\theta,\omega)$, which is angle of incidence θ dependent. The two quantities are related to impedance as follows, and coincide at normal incidence ($\theta = 0$):

$$\frac{1+R(\theta,\omega)}{1-R(\theta,\omega)} = \frac{1+W(\omega)}{1-W(\omega)}\cos\theta = \frac{Z(\omega)}{\rho c}\cos\theta \qquad (10)$$

In the previously studied special case of a well, the surface reflection kernel could be analytically identified as a delayed delta function and readily incorporated into the integration kernels. However for an arbitrary material this is not the case so an alternate strategy is required. Digital filtering of the surface sound discretisation coefficients offers a general purpose framework to implement arbitrary surface reflection processes, and is akin to the techniques used in recent FDTD algorithms [8,9,10]. Direct implementation of the convolution in equation 8 as a Finite Impulse Response FIR filter is computationally expensive, but use of a recursive Infinite Impulse Response (IIR) filter is an attractive option:

$$\varphi_{out}(\mathbf{x},t) * a^W(t) = \varphi_{in}(\mathbf{x},t) * b^W(t) \qquad (11)$$

The frequency domain surface reflection coefficient is a quotient of these two new functions and standard digital filter design techniques, such as the Impulse Invariant Method (IIM), may be used to find the digital filter tap values from Laplace domain material models:

$$W(s) = B^W(s)/A^W(s) \qquad (12)$$

4. Discretisation Scheme and Solver

In order to solve for the surface quantities numerically a discrete representation is required. The discretisation scheme uses a weighted sum of basis functions where the boundary is partitioned into planar elements over which pressure and particle velocity are considered spatially uniform within an instant and interpolated by a piecewise cubic polynomial in time [11,15]. Spatial resolution is defined by element size and temporal resolution by the time-step duration Δ_t. The incoming and outgoing waves are discretised separately, giving two sets of discretisation weights $\boldsymbol{\varphi}_j^{in}$ and $\boldsymbol{\varphi}_j^{out}$. This is in essence an indirect formulation and doubles storage and computation requirements, but the scaling of these costs with number of elements is unchanged.

In the Marching On in Time (MOT) solver, the discretisation weights are moved outside the integral of the KIE, creating a weighted sum of integrals that are dependent only on the surface geometry and independent of system excitation and boundary conditions. Upon evaluation these integrals become interaction coefficient matrices $\mathbf{Z}_l^{in}$ and $\mathbf{Z}_l^{out}$ that express scattered sound just from the discretisation weights, creating a matrix equation that is solved from known initial conditions. Causality dictates that past surface sound cannot be changed and future sound is irrelevant, hence at each time-step $t_j = j\Delta_t$ the algorithm is only solving for the current unknown weights. Because the surface model involves incoming and outgoing waves, each term appears twice (except the excitation vector $\mathbf{e}_j$):

$$\begin{aligned}&\mathbf{Z}_0^{in}\boldsymbol{\varphi}_j^{in} + \mathbf{Z}_0^{out}\boldsymbol{\varphi}_j^{\mathrm{out}} \\ &= \mathbf{e}_j - \textstyle\sum_{l=1}^{N_l}\left[\mathbf{Z}_l^{in}\boldsymbol{\varphi}_{j-l}^{in} + \mathbf{Z}_l^{out}\boldsymbol{\varphi}_{j-l}^{\mathrm{out}}\right]\end{aligned} \qquad (13)$$

This matrix equation has twice as many unknowns as rows and hence cannot be solved on its own and the surface reflectance relationship must also be utilized. Accordingly, equation 11 is re-written with the convolutions replaced by discrete expressions involving the element under consideration's discretisation weights:

$$\textstyle\sum_{l=0}^{N_a} a_l\varphi_{j-l}^{out} = \sum_{l=0}^{N_b} b_l\varphi_{j-l}^{in} \qquad (14)$$

This is combined into the MOT solver matrix in equation 15 below, where the matrices $\mathbf{A}_l$ and $\mathbf{B}_l$ contain the filter tap values (equation 14) for all the elements along their diagonals. Unlike the case of coupling IIR boundary filters to FDTD where extra code and memory is required to

$$\begin{bmatrix}\mathbf{Z}_0^{in} & \mathbf{Z}_0^{out}\\ -\mathbf{B}_0 & \mathbf{A}_0\end{bmatrix}\begin{bmatrix}\boldsymbol{\varphi}_j^{in}\\ \boldsymbol{\varphi}_j^{out}\end{bmatrix} = \begin{bmatrix}\mathbf{e}_j\\ \mathbf{0}\end{bmatrix} - \textstyle\sum_{l=1}^{N_l}\begin{bmatrix}\mathbf{Z}_l^{in} & \mathbf{Z}_l^{out}\\ -\mathbf{B}_l & \mathbf{A}_l\end{bmatrix}\begin{bmatrix}\boldsymbol{\varphi}_{j-l}^{in}\\ \boldsymbol{\varphi}_{j-l}^{out}\end{bmatrix} \qquad (15)$$

handle them as a special case, here the digital filtering has been incorporated directly into the standard BEM solution framework, with no solver modifications necessary. If desired the system may be readily recast to solve for pressure and normal velocity as discretised unknowns, just by applying a simple matrix transformation to the interaction matrices, in which case impedance boundary conditions in the form of equation 7 may be implemented directly. As this amounts to just scaling and addition of rows, identical numerical results are produced with no change to the condition number of the matrices or stability of the time-marching system. This result is in stark disagreement to some of the FDTD literature, where surface impedance and surface reflectance based boundary conditions are believed to be based on fundamentally different assumptions, and the latter only ever accurate for certain angles of incidence [10].

It is also interesting to note that, while this is currently a locally reacting surface model, it should be possibly to incorporate extended reaction just by including off-diagonal terms in $\mathbf{A}_l$ and $\mathbf{B}_l$; for example these could be replaced by stiffness matrices to couple to a simple FEM model of membrane motion [9].

5. Results

The test geometry studied aimed to replicate the scenarios used to test the performance of digital filter boundary conditions in the FDTD literature (specifically the work published by the Sonic Arts Research Centre, Belfast [8]), where the pressure reflection coefficient is calculated for plane waves incident from various angles onto a homogenous planar sample of the material under study. Ideally the sample would be of infinite extent to remove edge diffraction, but that is not tractable so instead a finite sample is simulated and the late arriving effects of the truncation are time-windowed out. The model differs from those used in FDTD in the following ways:

- Only the surface need be modelled, so treatments to deal with finite simulation volumes are not needed.
- Incident and scattered pressure are calculated separately at points in the volume, so subtraction of multiple simulations is not necessary.
- True plane-wave sources are possible, so approximation by a distant point source is not necessary.

Because diffraction from the surface edge will travel tangentially along the surface, it is necessary to model a greater area in the direction the plane wave originated from as excitation arrives there earlier. The zone contributing within a given time was found to always be an ellipse (figure 1), but this differed for every incidence angle so the mesh was made to be a simple bounding rectangle. A 4m by 8.8m plane gave a 5.8ms analysis window (58 samples at Δ_t=0.1ms) for incident angles up to 45° and required 8775 0.1m×0.1m surface elements (with symmetry). More tangential angles were not modelled due to an increased element count beyond the available hardware capabilities. The two receivers (●) were located 0.1m from either side of the surface. The source signal was a Gaussian pulse in velocity potential (so a Ricker wavelet in pressure) with its standard deviation set to $2\Delta_t$; this contained significant energy up to 2.5kHz.

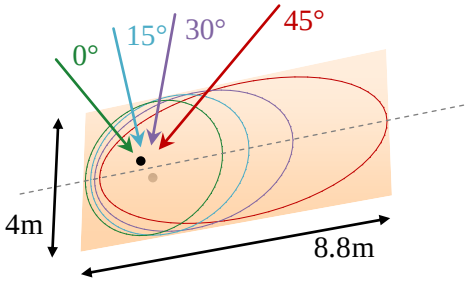

Figure 1. Geometry of the planar sample, including plane wave arrival directions & contributing zones

Figure 2 shows compares the pressure reflection coefficient for the rigid boundary condition $w(t) = \delta(t)$ calculated analytically (equation 10) and numerically using time domain BEM. Note that in the rigid case the analytical results are identical for all angles so are superimposed. These results were numerically identical to those achieved using a rigid-surface variant of the BEM code, so do not include any error arising from the boundary condition model and may be considered as a benchmark for comparison with the following results. The error between the curves fits with the expected trend, being very small at low frequencies and becoming more significant at higher frequencies. The time-step was chosen to be slightly explicit, to achieve the best ratio of time window length to surface element count, and the "8 elements per wavelength" rule is satisfied up to 428Hz or 1250Hz by considering element size or time-step duration respectively.

Figure 3 presents the same quantities for a "welled surface" boundary condition as studied in [15]. In this case the well depth was chosen to be half the

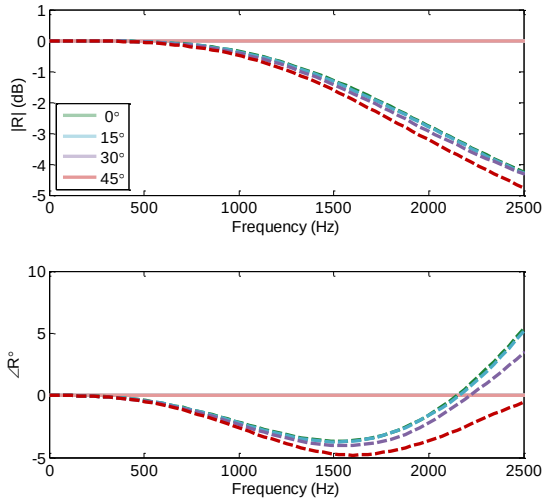

Figure 2. Pressure reflection coefficient for a rigid boundary (analytical ▬ numerical ▪▪▪)

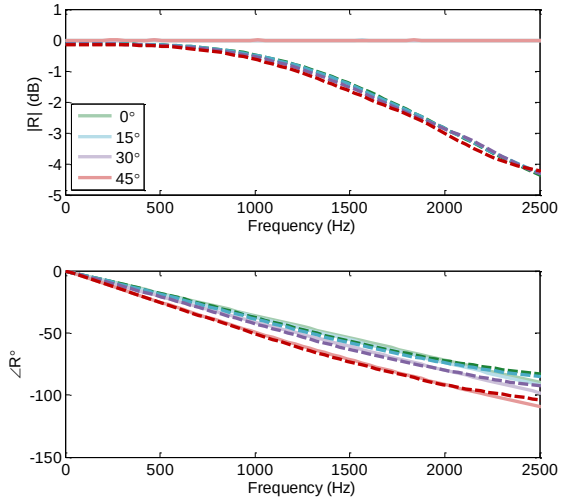

Figure 3. Pressure reflection coefficient for a welded boundary (analytical ▬ numerical ▪▪▪)

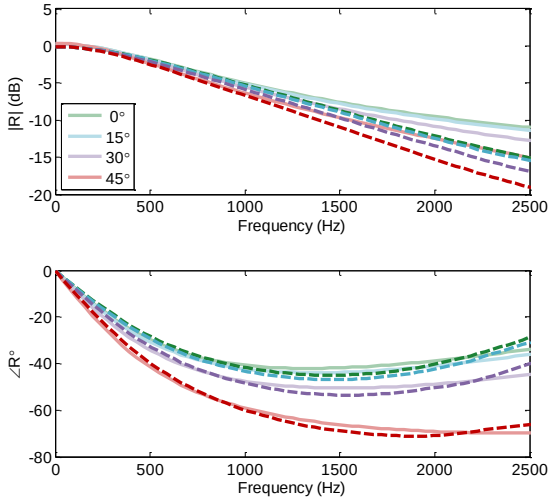

Figure 4. Pressure reflection coefficient for a low-pass reflectance boundary (analytical ▬ numerical ▪▪▪)

distance sound travelled in a time-step, so $w(t) = \delta(\Delta_t)$. The delay causes a linear-phase trend with some incidence angle dependence but no magnitude change. The error between this and the numerical result differs little from that seen in figure 2, so may be attributed to factors other than the boundary condition implementation.

Figure 4 shows results from modelling the low-pass reflectance boundary studied in [8]. Such a boundary condition may seem unrealistic, but in fact this is the general trend seen for many common acoustic treatments such as porous absorbent. The exact definition is a single pole recursive filter defined by $W(s) = g\alpha/(s + \alpha)$, where s has been normalised to the sampling frequency and g and α equal 0.85 and 0.4 respectively. Error here follows the same trends, except that there is an additional slight discrepancy in magnitude at 0Hz. This is due to the time-window slightly truncating the impulse response of the boundary filter, and becomes more significant for higher-order filters with lower cut-offs which have correspondingly longer impulse responses. However this is an error due to limitations of the comparison scheme and the boundary implementation still appears to be working well.

Figure 5 shows results from modelling the mechanical boundary studied in [8]. This is a mass-spring-damper system and may be considered as an idealised model of membrane motion in panels or Helmholtz absorbers. The reflectance filter was defined by its impedance $Z(s) = \rho c(Ms^2 + Rs + K)/s$, where $M = 6\Delta_t$, $R = 2$ and $K = 2/\Delta_t$. This was mapped to the digital domain specification using the IIM on specific surface admittance (the reciprocal of impedance normalised by ρc) and implemented using the form of equation 7, with surface pressure and particle velocity as the solver unknowns.

A resonance exists just below 1kHz and this causes increased absorption as sound energy is lost by coupling into the mechanical resistance. This appears as a dip in reflection magnitude and associated change in phase. In addition to the error effects described previously it seems that this dip is less emphasised in the numerical model than the analytical result suggest it should be. This could again be due to the time-window truncating the slowly decaying part of the impulse response that oscillates at this frequency, the frequency domain counterpart of which would be spectral

smearing of neighbouring frequencies into the attenuation band. The error is more significant at larger angles, which suggests that spatial resolution could also be a compromising factor. Further experimentation is required to confirm that these artefacts are due to the verification process and that the boundary condition model operates correctly.

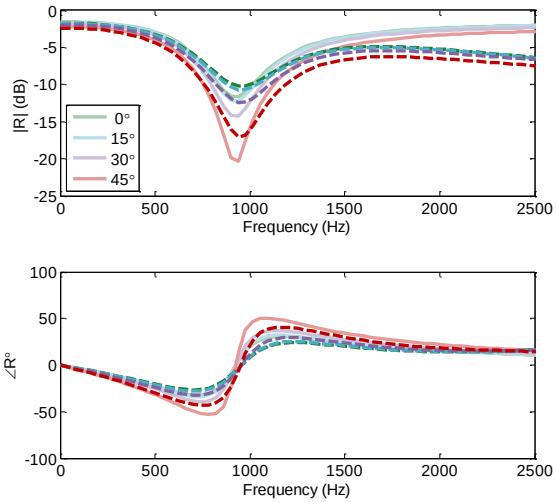

Figure 5. Pressure reflection coefficient for a mechanical boundary (analytical ▬ numerical ▪▪▪)

6. Conclusions

This paper aimed to propose a boundary condition model for the time domain Boundary Element Method which would achieve the same extent of applicability and accuracy as surface impedance does for the frequency domain BEM. A digital filter based scheme was devised which allows either surface reflectance or surface impedance to be implemented directly with exact numerical equivalence. This contradicts opinion stated in some of the FDTD literature, where it is reported that surface reflectance based boundary conditions are only ever accurate for certain angles of incidence.

Results were presented for four different boundary conditions applied to a flat homogeneous plane designed to mimic the test scenarios used for this purpose in the FDTD literature. Some error was observed, but this seemed attributable either to the discretisation error in the time domain BEM algorithm or windowing error in the verification process. The boundary condition model did not appear to be a source of additional error and produced trends matching the analytical reflection coefficient at a variety of angles.

References

[1] T. J. Cox and Y. W. Lam: "Prediction and Evaluation of the Scattering from Quadratic Residue Diffusers", J. Acoust. Soc. Am. Vol. 95 (1), 1994, pp. 297-305

[2] M. B. Friedman and R. P. Shaw, "Diffraction of Pulses by Cylindrical Obstacles of Arbitrary Cross Section", J. Appl. Mech. Vol. 29, 1962, pp. 40 – 46

[3] T. Abboud, M. Pallud, and C. Teissedre, "SONATE: a Parallel Code for Acoustics" http://imacs.xtec.polytechnique.fr/Reports/sonate-parallel.pdf

[4] T. Ha-Duong, B. Ludwig and I.Terrasse, "A Galerkin BEM for transient acoustic scattering by an absorbing obstacle", Int. J. Numer. Meth. Engng. Vol. 57, 2003, pp. 1845 – 1882

[5] P. H. L. Gronenboom, "The applications of boundary elements to steady and unsteady potential fluid flow problems in two and three dimensions", Appl. Math. Modelling Vol. 6, 1982. pp. 35 – 40

[6] R. P. Shaw, "Diffraction of Acoustic Pulses by Obstacles of Arbitrary Shape with a Robin Boundary Condition", J. Acoust. Soc. Am. Vol. 41 (4A), 1967, 855 – 859

[7] C. K. W. Tam and L. Auriault, "Time-Domain Impedance Boundary Conditions for Computational Aeroacoustics", AIAA J. Vol. 34 (5) 1996, 917 – 923

[8] K. Kowalczyk and M. Van Walstijn, "Modelling Frequency-Dependent Boundaries as Digital Impedance Filters in FDTD and K-DWM Room Acoustics Simulations" J. AES, Vol. 56 (7/8), 2008, pp. 569 – 583

[9] I. A. Drumm and Y. W. Lam: "Development and assessment of a finite difference time domain room acoustic prediction model that uses hall data in popular formats", Proceedings, Internoise-Turkey, (2007)

[10] J. Escolano, J. J. López and B. Pueo, "Locally Reacting Impedance in a Digital Waveguide Mesh by Mixed Modeling Strategies for Room Acoustic Simulation", Acta Acustica united with Acustica, Vol. 95 (6), 2009, pp. 1048 – 1059

[11] A. A. Ergin, B. Shanker and E. Michielssen, "Analysis of transient wave scattering from rigid bodies using a Burton-Miller approach", J. Acoust. Soc. Am. Vol. 106 (5), 1999, pp. 2396 – 2404

[12] D. J. Chappell, P. J. Harris, D. Henwood and R. Chakrabarti, "A stable boundary integral equation method for modelling transient acoustic radiation", J. Acoust. Soc. Am. Vol. 120 (1), 2006, 74 – 80

[13] A. J. Burton and G. F. Miller, "The application of integral equation methods to the numerical solution of some exterior boundary-value problems", P. Roy. Soc. Lond. A. Mat. Vol. 323, 1971, pp. 201 – 210

[14] K.-Y. Fung, H. Ju, B.-P. Tallapragada, "Impedance and Its Time-Domain Extensions", AIAA J. Vol. 38 (1), 2000, pp. 30 – 38

[15] J. A. Hargreaves and T. J. Cox, "A transient boundary element method model of Schroeder diffuser scattering using well mouth impedance", J. Acoust. Soc. Am. Vol 124 (5), 2008, pp. 2942 – 2951